nature photonics

Article

https://doi.org/10.1038/s41566-025-01756-4

Universal routing of light via optical thermodynamics

Received: 25 December 2024

Accepted: 7 August 2025

Published online: 25 September 2025

Check for updates

Hediyeh M. Dinani[1,4], Georgios G. Pyrialakos[1,4], Abraham M. Berman Bradley[1], Monika Monika[2], Huizhong Ren[1], Mahmoud A. Selim[1], Ulf Peschel[2], Demetrios N. Christodoulides[1,3] & Mercedeh Khajavikhan[1,3]

Understanding and exploiting the dynamics of complex nonlinear systems is nowadays at the core of a broad range of scientific and technological endeavours. Within the optical domain, light evolution in a nonlinear multimode environment presents a formidable problem, as its chaotic evolution often hinders predictive insights. Recently, an optical thermodynamic framework has been put forward that, in a systematic manner, can not only predict but also harness the intricate behaviour of these systems. By deploying entropic principles, here we demonstrate a counter-intuitive optical process in which light, launched into any input port of a judiciously designed nonlinear array, universally channels into a tightly localized ground state, a response that is completely unattainable in linear conservative arrangements. This phenomenon arises from the interplay between lattice structure and the way the kinetic and nonlinear Hamiltonian components unfold, leading to two optical thermal processes: Joule–Thomson-like expansion followed by mode thermalization. Experimentally, this effect is demonstrated in properly configured nonlinear time-synthetic mesh lattices, where the optical temperature approaches near zero, causing light to condense at a single spot, regardless of the initial excitation position. The effect demonstrated here opens new avenues for applying the principles of optical thermodynamics in realizing new optical functionalities, such as all-optical beam-steering, multiplexing and nonlinear beam-shaping in high-power regimes, while also offering a greater understanding of the notable physics of light–matter interactions in multimode nonlinear systems.

Chaotic dynamics are a defining feature of complex systems across various fields, ranging from turbulent particle interactions in gases[1,2] to phase transitions in magnetic materials[3–5] and protein-folding in biological systems[6,7]. Multimode optical arrangements present a similarly intricate landscape, where nonlinearities intertwine several degrees of freedom, leading to complex and seemingly unpredictable wave dynamics[8–12]. Despite their perplexing nature, these photonic systems hold promise for revealing new, uncharted behaviours, suggesting realms previously considered beyond reach. Lately, a self-consistent optical thermodynamic framework grounded in entropic principles[13–15] has been developed to address these complexities. Just as classical thermodynamics[16] has driven transformative advancements—enabling the design of heat engines, the prediction of phase transitions[17] and the understanding of energy flow from biological to cosmological systems[18]—this methodology provides similar predictive capabilities for complex light dynamics through universal laws and macroscopic parameters such as optical temperature and entropy[19–31].

A full list of affiliations appears at the end of the paper. e-mail: demetri@usc.edu; khajavik@usc.edu

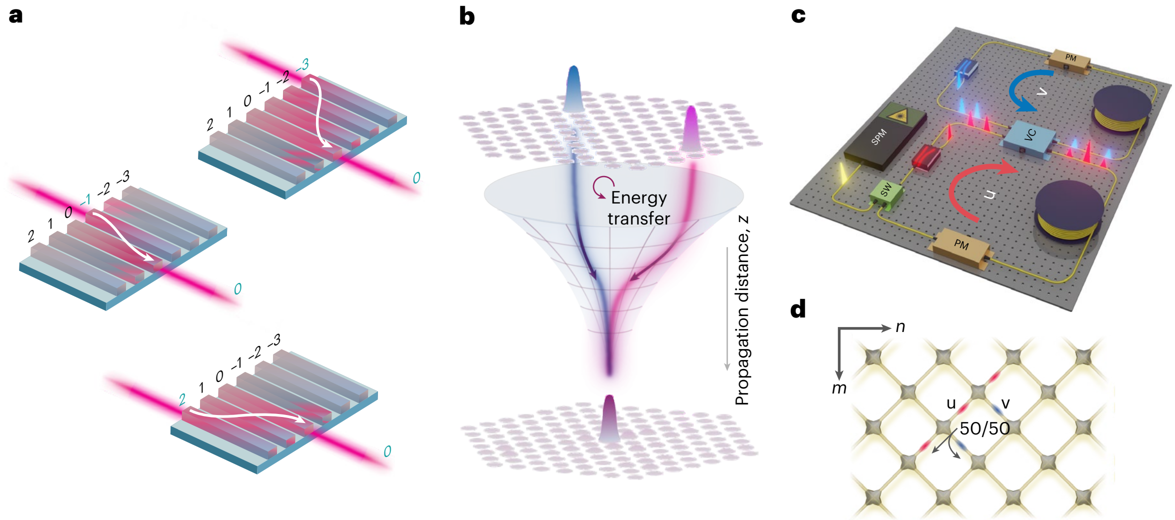

Fig. 1 | Nonlinear funnelling of light. a, Conceptual illustration of a photonic integrated array, engineered to universally route light into its central port. This dynamic response is prohibited in linear, conservative systems. **b**, Simulation results of funnelling in a nonlinear 37-core coupled array, when excited simultaneously at two independent ports, with normalized power $P = 10.5$ per port. The lattice exhibits a conical potential with a normalized detuning difference $\Delta_c - \Delta_o = 6$ between the outermost elements (Δ_o) and the central site (Δ_c). **c**, The simplified experimental set-up consists of two nonlinear optical fibre loops of unequal length connected by a variable coupler. Each loop contains a phase modulator to control the real part of the lattice potential. The short loop is connected to a pulse source generator (seed pulse module) through an optical switch. During propagation, the pulse intensities are monitored by photodetectors. **d**, The pulse propagation dynamics through the short (u; red) and long (v; blue) fibre loops can be mapped onto a mesh lattice of beam splitters as a function of position n and round trip m (see Supplementary Information Section II for details). PM, phase modulator; SPM, seed pulse module; SW, optical switch; VC, variable coupler.

In this work, we leverage tenets from statistical physics to demonstrate efficient and universal light-routing in conservative nonlinear waveguide arrays. This process allows light to reliably reach a designated output channel, regardless of its entry port to the array (Fig. 1a,b). We note that under linear conditions, this functionality is unattainable without employing significant levels of gain, especially as the number of input ports increases[32,33]. In other words, it is impossible to conceive of a unitary transformation that enables efficient light transport from a multitude of input sites (when excited one at a time) to a pre-assigned exit port, as this would violate reciprocity[33]. Nonlinearity could, perhaps, overcome this fundamental hurdle; however, the appropriate strategy for achieving this goal remains unclear. As we will see, this elusive funnelling capability can be achieved through a Joule–Thomson (JT) exchange[29] between the photonic kinetic and nonlinear Hamiltonian components of the system, resulting in rapid cooling of light to a near-zero optical temperature, followed by mode thermalization. This effect emerges in conservative potential landscapes that favour localized lower-order states on one side of the lattice while supporting a set of extended modes in the bulk. Clearly, the realization of universal funnelling methodologies could enhance the arsenal of tools available in photonics that are aimed at controlling and manipulating the flow of light[34–42]. In the following, we will experimentally demonstrate this behaviour using a nonlinear photonic time-synthetic optical mesh-lattice platform[19,32] (Fig. 1c,d).

To exemplify this intriguing prospect, we perform simulations in a prototypical one-dimensional discrete Kerr nonlinear array[43] with triangular on-site energies. This lattice closely mirrors the mesh-lattice environment used in our experiments (Fig. 2a). In this arrangement, the complex optical field state vector $|\Psi\rangle$ evolves according to $\mathrm{i}\frac{\mathrm{d}|\Psi\rangle}{\mathrm{d}z} + (\widehat{H}_\mathrm{L} + \widehat{H}_\mathrm{NL})|\Psi\rangle = 0$, where $\widehat{H}_\mathrm{L}$ is a normalized Hermitian matrix comprising off-diagonal nearest-neighbour coupling elements as well as local (diagonal) detunings or energies Δ_n, whereas the diagonal operator $\widehat{H}_\mathrm{NL}$ accounts for the Kerr nonlinearity. In general, the state vector of $|\Psi\rangle$ can be projected onto the linear supermodes $|u_i\rangle$ of the system ($\widehat{H}_\mathrm{L}\,|u_i\rangle = \varepsilon_i\,|u_i\rangle$) having eigenvalues ε_i, in which case $|\Psi\rangle = \sum_i c_i\,|u_i\rangle$ where c_i represents the respective complex mode coefficient. In conservative optical multimode settings, nonlinearity induces a chaotic and, thus, ergodic energy exchange among the modal occupancies $|c_i(z)|^2$, an effect that underlies their thermodynamic response. These statistical processes are governed by two constants of motion: the total Hamiltonian energy $H_\mathrm{tot} = H_\mathrm{L} + H_\mathrm{NL}$, which involves both a linear and a nonlinear component, and the total optical power $P = \sum_i |c_i(z)|^2$. The linear part of the Hamiltonian, $H_\mathrm{L} = -U = \sum_i \varepsilon_i\,|c_i(z)|^2$, is associated with the 'kinetic' energy of the system, whereas the nonlinear contribution, $H_\mathrm{NL} = (1/2)\sum_n |a_n(z)|^4$ (ref. 43; expressed in the local basis $|\Psi\rangle = (a_1, \ldots, a_n)$), represents a nonlinear interaction energy. To facilitate a funnelling path through thermodynamics, the array is designed with highly localized lower-order modes confined to one side, while higher-order (bulk) modes remain extended throughout the lattice. This is achieved by progressively adjusting the detuning between individual sites at a constant rate $\delta\Delta$ ($\delta\Delta = \Delta_n - \Delta_{n-1}$), thereby forming a truncated triangular discrete potential in this one-dimensional arrangement (Fig. 2a). The same methodology applies to two-dimensional lattices, where the local energies assume a conical-like profile (Fig. 1b).

The thermal aspects of this funnelling process are illustrated in Fig. 2b. A high-intensity signal or beam is injected into this triangular potential lattice. From an energetic perspective, the system is initially dominated by a nonlinear Hamiltonian component H_NL, which happens to be in a superposition of many higher-order modes. As the light packet evolves in the lattice, it gradually sheds some energy because of Peierls–Nabarro effects[44], thus forming a moderately confined, discrete soliton-like entity[43,45], which, like a particle, continuously accelerates (Fig. 2b) within the linear (biased) potential lattice[46]. As a result, the modal content of the soliton beam progressively changes (Fig. 2c) while its kinetic energy $|U|$ steadily increases at the expense of the nonlinear component (Fig. 2d). At this stage, light behaves non-thermally, and the dynamics cannot yet be described within the framework of optical thermodynamics. We note that our lattice is deliberately designed to display a small step $\delta\Delta$ to suppress Bloch oscillations[47,48] through the action of nonlinearity. Eventually, this

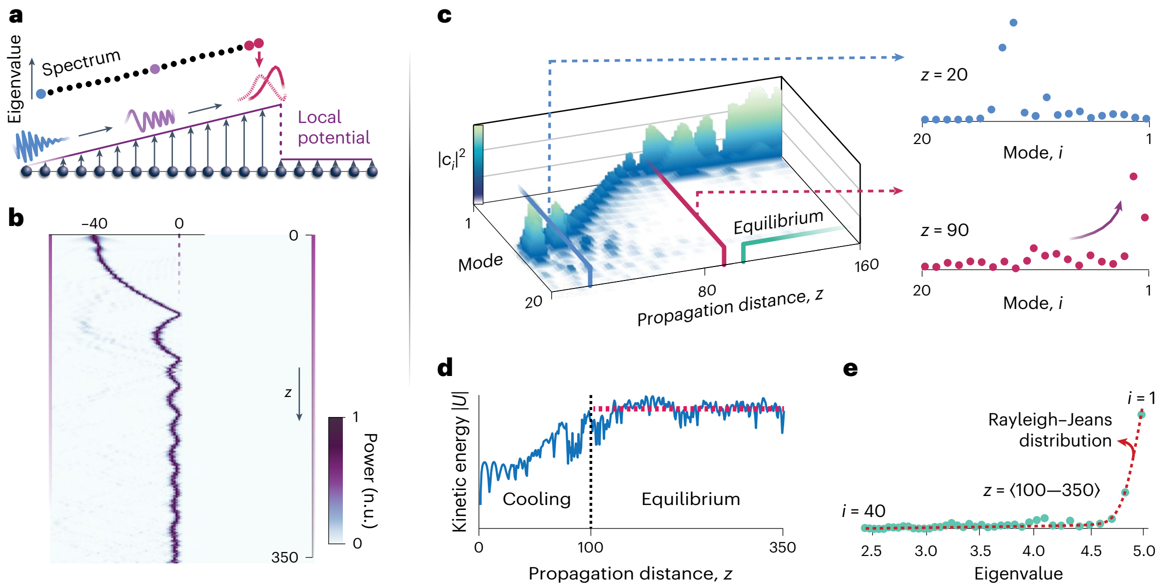

Fig. 2 | Thermodynamic principle of light-funnelling. **a**, A coupled array system with its lower-order modes (red) localized at the peak of its weakly truncated triangular potential. **b**, Within an appropriate range of potential slopes, the funnelling regime becomes accessible. Here, a lattice with $\delta\Delta = 0.02$ and peak site at 0 is excited at the port −40 with normalized power $P = 4$. **c**, Evolution of modal amplitudes during funnelling for the scenario depicted in **b**. The wave packet undergoes optical cooling, progressively carrying power towards the lower-order modes. **d**, During this process the kinetic energy increases. **e**, A Rayleigh–Jeans distribution manifests at equilibrium (here depicted as a time average of the modal amplitudes for 250 time steps). The theoretical red dashed curve in **e** was calculated using the mean equilibrium value of U (red continuous line in **d**). n.u., normalized units.

soliton state reaches the end of the triangular array where the lowest-order mode resides. Here, the abrupt collision leads to a series of reflections, causing the beam to completely disintegrate into a low-temperature 'gas' state, where the Hamiltonian energy is almost entirely converted into kinetic U, which remains quasi-invariant thereafter. Beyond this point, the photon gas enters a second weakly nonlinear phase where it attains thermal equilibrium, as revealed by the emergence of a Rayleigh–Jeans distribution (Fig. 2e). At this stage, the expectation value of the modal content is given by $\langle |c_i|^2 \rangle = -\frac{T}{\varepsilon_i + \mu}$, where T is the optical temperature and μ the chemical potential[13,20–22,28]. This all-optical energy transformation process, akin to JT expansion[29] encountered in standard statistical mechanics[16], is the driving mechanism for the light-funnelling discussed in this work. For the example provided here, the final temperature is exceedingly low ($T = 0.012$), indicating, indeed, that the optical energy predominantly occupies the ground state (Fig. 2e). Importantly, this effect is independent of the input, as the optical energy is faithfully funnelled into the highly localized fundamental mode of the system, regardless of the excitation site (Supplementary Information Section IX).

To experimentally demonstrate light-funnelling in a nonlinear lattice environment, we designed a nonlinear fibre loop set-up (Fig. 1c) that allows one to observe the evolution of light packets in discrete time steps[19] (Supplementary Information Section I). Our set-up consists of two ~3-km-long dispersion-compensating fibre loops exhibiting an appreciable Kerr nonlinearity. The loops are slightly unequal in length (~20 m). These loops are coupled together by a variable coupler, effectively establishing a one-dimensional lattice with the same nearest-neighbour coupling (Supplementary Information Section II). A 20-ns pulse from a highly coherent distributed-feedback laser is subsequently injected into one of the loops through an optical switch (Fig. 1c). Using a time-multiplexing scheme, pulse sequences travelling in the short (u) and long (v) loops are temporally advanced and delayed, respectively, resulting in discrete time slots (synthetic positions n) within each round trip (time step m), as shown in Fig. 1d. During this process, the pulses accumulate a nonlinear phase[49]. The use of two phase modulators, one in each loop, allows us to realize a triangular potential at each site n that reaches a height of 0.324π. Given that the lattice involves 52 sites (or supermodes), the site-to-site phase difference is $\delta\varphi = \varphi(n, m) - \varphi(n-1, m) = 0.0062\pi$.

In our experiments, funnelling was observed when the injected pulse peak power was around ~160 mW and after approximately $m = 100$ time steps. Figure 3a illustrates the experimentally observed light evolution in a triangular potential lattice when a signal is injected at the $n = -10$ site of the short loop (u). In line with the preceding theoretical discussion, as the pulse traverses the array, it initially forms a soliton-like state after some readjustment. This self-confined state then accelerates, as indicated by its parabolic trajectory (Fig. 3a), within the time interval $0 \le m \lesssim 80$, eventually striking the truncated triangular barrier and undergoing a series of self-bouncing reflections lasting up to $m \approx 125$. This initial cooling phase is characterized by two crucial aspects: (1) a continuous shift in the eigenfunctions constituting the beam, ultimately engaging primarily the fundamental mode located at the peak of the triangular potential, and (2) an increase in the kinetic energy component U (Fig. 3c), which progressively approaches the value $U \approx -\varepsilon_1 P_1$, where ε_1 and P_1 represent the eigenvalue and power associated with the ground state, respectively[29]. The behaviour displayed in Fig. 3a is in excellent agreement with numerical simulations (Fig. 3b). Beyond $m \approx 100$, the soliton fragments undergo JT thermalization, resulting in a cooled Rayleigh–Jeans distribution (Fig. 3d) having a normalized optical temperature of $T = 0.004$ and a chemical potential $\mu = -2.38$, indicating that most of the power occupies the fundamental mode. To demonstrate the robustness of this process, we further examine the behaviour of the system under excitation from different sites. The experimental results for input locations $n = -20$ and $n = -30$ in the short (u) loop, along with the corresponding light evolution simulations, are presented in Fig. 3e,f, respectively. When the injection site is further from the centre, higher-order modes, which tend to spread towards the edges of the lattice, are preferentially excited. This results in a slightly slower progression of the optical cooling process. Here, the transition from JT expansion to optical thermalization occurs at around $m \approx 120$, as the system requires more time to redistribute its

https://doi.org/10.1038/s41566-025-01756-4

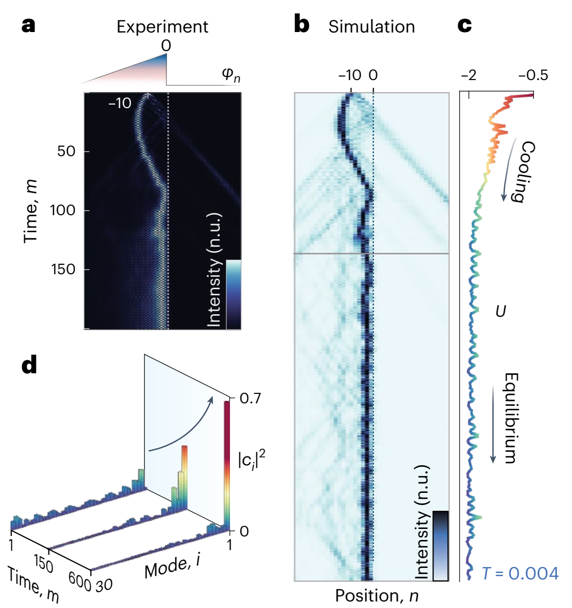

Fig. 3 | Experimental observation of universal light-funnelling. **a**,**b**, Experimental data (**a**) and corresponding simulation (**b**) depicting the evolution of a single pulse injected at a power level of 160 mW at position $n = -10$ in the short loop, within a triangular-shaped potential that abruptly drops at the centre of the lattice. **c**, The monotonic increase in the optical kinetic energy U during propagation indicates that the photon gas has transitioned from a 'hot' state to a near-zero optical temperature. **d**, The modal occupancy is monitored at three specific time steps ($m = 1$, 150 and 600) by projecting the field onto the lattice supermodes, demonstrating a power transfer to the fundamental mode. **e**,**f**, Experimental results regarding the impact that the initial injection position has on the funnelling process, obtained at $n = -20$ (**e**) and −30 (**f**). The measured pulse intensities are normalized at each time step.

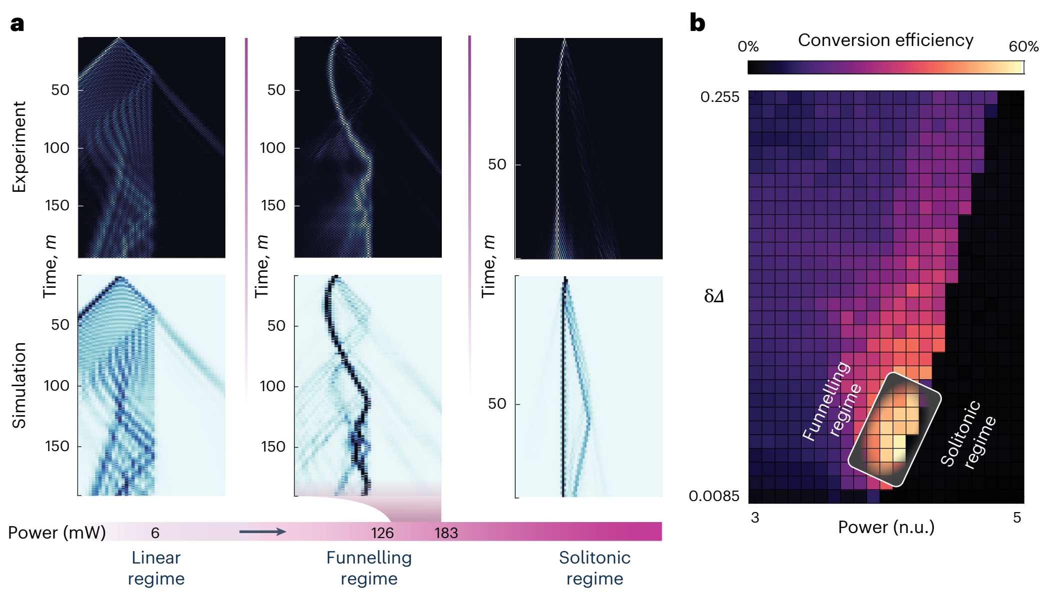

Fig. 4 | Regime of optical funnelling. **a**, Left: under weak nonlinear conditions, a diffraction pattern is manifested. Middle: at a higher power level, a moderately confined soliton emerges, which funnels to a designated output port. Right: at higher power levels, a strong soliton is formed, which charts its trajectory. **b**, Funnelling efficiency map as a function of normalized power and detuning slope difference $\delta\Delta$. The region exhibiting efficient funnelling is marked by the box. It borders the solitonic regime.

energy towards the lower-order modes near the peak of the triangular potential. Nonetheless, in both cases, the system guides light towards the fundamental mode as expected from a universal router. More results, along with findings that further confirm the universality of this process, are provided in Supplementary Information Sections VI and IX.

Light-funnelling, as described above, arises from the intricate dynamics of moderately nonlinear multimode systems, whose behaviour markedly differs from both linear arrays and highly nonlinear scenarios. As a result, for a given potential landscape, universal routing occurs within a certain range of optical powers. At low power levels, the system operates in a quasi-linear regime that, in principle, in large arrays, can display weakly interacting Bloch oscillations[47,48]. These oscillations tend to disperse light across several sites, thus preventing the emergence of power-siphoning behaviour (Fig. 4a, first panel). As the injected power increases, nonlinear phase accumulation takes over, gradually suppressing these oscillations and establishing a moderately confined accelerating soliton state. This, in turn, enables a funnelling regime where light is efficiently directed towards the designated output site through JT cooling and mode equilibration (Fig. 4a, middle panel). Across this power range, universal routing is consistently observed in all trials, demonstrating the robustness of this mechanism. At higher power levels, the system enters a strongly nonlinear regime where strong soliton self-focusing overrides the influence of the potential because of pronounced Peierls–Nabarro effects[44]. In this state, a highly localized discrete soliton[43] forms that charts independent trajectories around the excited site, once again preventing the funnelling behaviour from occurring (Fig. 4a, right panel). Figure 4b further illustrates the efficiency of universal routing as a function of the potential slope of the array and the input power, revealing a transition between the solitonic and funnelling regimes. It is important to note that the nonlinear dynamics considered here is inherently Liouvillian and subject to time-reversal symmetry. However, any deviation from a perfectly phase-conjugated output is expected to result in significantly different initial conditions at the input, due to the chaotic dynamics unfolding in this complex arrangement. Consequently, although the system is, in principle, time-reversible, the universal routing behaviour is expected to be practically irreversible, much like in an actual thermodynamic environment (Supplementary Information Section XII).

In conclusion, we have demonstrated a new nonlinear light-routing mechanism, where optical signals, regardless of their entry point, are directed to converge at a designated output port. This intriguing behaviour arises from the interplay between the modal structure of the array and two distinct optical thermodynamic processes enabled by the multimode nonlinear environment: a JT-like expansion facilitating optical cooling followed by thermalization, which equilibrates the light into a Rayleigh–Jeans distribution, ultimately concentrating it into the ground state of the lattice. The principles unveiled here can be extended to other photonic platforms, such as integrated nonlinear waveguide arrays and photonic crystal multicore fibres, where similar funnelling schemes could have transformative applications in optical spatial multiplexing systems, beam-shaping and power-scaling. Furthermore, our findings highlight the value of optical thermodynamics in identifying new regimes of light–matter interactions in nonlinear multimode systems, thus offering fresh insights into the dynamics of complex optical arrangements and advancing their potential for high-power applications.

Online content

Any methods, additional references, Nature Portfolio reporting summaries, source data, extended data, supplementary information, acknowledgements, peer review information; details of author contributions and competing interests; and statements of data and code availability are available at https://doi.org/10.1038/s41566-025-01756-4.

References

1. Wit, X. M., Fruchart, M., Khain, T., Toschi, F. & Vitelli, V. Pattern formation by turbulent cascades. *Nature* **627**, 515–521 (2024).
2. Manneville, P. *Instabilities, Chaos and Turbulence*, Vol. 1 (World Scientific, 2010).
3. Pelissetto, A. & Vicari, E. Critical phenomena and renormalization-group theory. *Phys. Rep.* **368**, 549–727 (2002).
4. Wigen, P. E. *Nonlinear Phenomena and Chaos in Magnetic Materials* 1–12 (World Scientific, 1994).
5. Deng, S. et al. Phase transitions associated with magnetic-field induced topological orbital momenta in a non-collinear antiferromagnet. *Nat. Commun.* **15**, 822 (2024).
6. Uversky, V. N. Dancing protein clouds: the strange biology and chaotic physics of intrinsically disordered proteins. *J. Biol. Chem.* **291**, 6681–6688 (2016).
7. Jumper, J. et al. Highly accurate protein structure prediction with AlphaFold. *Nature* **596**, 583–589 (2021).
8. Boyd, R. W. & Gaeta, A. L. in *Laser Optics of Condensed Matter, Vol. 2, The Physics of Optical Phenomena and Their Use as Probes of Matter* (eds Garmire, E. et al.) 99–105 (Springer, 1991).
9. Zakharov, V. E., L'vov, V. S. & Falkovich, G. *Kolmogorov Spectra of Turbulence I: Wave Turbulence* (Springer, 2012).
10. Mangini, F., Ferraro, M., Tonello, A., Couderc, V. & Wabnitz, S. High-temperature wave thermalization spoils beam self-cleaning in nonlinear multimode GRIN fibers. *Opt. Lett.* **48**, 4741–4744 (2023).
11. Longhi, S. Modulational instability and space time dynamics in nonlinear parabolic-index optical fibers. *Opt. Lett.* **28**, 2363–2365 (2003).
12. Mangini, F. et al. Statistical mechanics of beam self-cleaning in GRIN multimode optical fibers. *Opt. Express* **30**, 10850–10865 (2022).
13. Wu, F. O., Hassan, A. U. & Christodoulides, D. N. Thermodynamic theory of highly multimoded nonlinear optical systems. *Nat. Photonics* **13**, 776–782 (2019).
14. Parto, M. et al. Thermodynamic conditions governing the optical temperature and chemical potential in nonlinear highly multimoded photonic systems. *Opt. Lett.* **44**, 3936–3939 (2019).
15. Makris, K. G. et al. Statistical mechanics of weakly nonlinear optical multimode gases. *Opt. Lett.* **45**, 1651–1654 (2020).
16. Pathria, R. K. & Beale, P. D. in *Statistical Mechanics* 1–23 (Elsevier, 2011).
17. Martynov, G. A. The problem of phase transitions in statistical mechanics. *Phys.-Uspekhi* **42**, 517 (1999).
18. Bekenstein, J. D. Generalized second law of thermodynamics in black-hole physics. *Phys. Rev. D* **9**, 3292 (1974).
19. Marques Muniz, A. L. et al. Observation of photon-photon thermodynamic processes under negative optical temperature conditions. *Science* **379**, 1019–1023 (2023).
20. Pourbeyram, H. et al. Direct observations of thermalization to a Rayleigh-Jeans distribution in multimode optical fibres. *Nat. Phys.* **18**, 685–690 (2022).
21. Mangini, F. et al. On the maximization of entropy in the process of thermalization of highly multimode nonlinear beams. *Opt. Lett.* **49**, 3340–3343 (2024).
22. Fusaro, A., Garnier, J., Krupa, K., Millot, G. & Picozzi, A. Dramatic acceleration of wave condensation mediated by disorder in multimode fibers. *Phys. Rev. Lett.* **122**, 123902 (2019).
23. Pyrialakos, G. G., Ren, H., Jung, P. S., Khajavikhan, M. & Christodoulides, D. N. Thermalization dynamics of nonlinear non-Hermitian optical lattices. *Phys. Rev. Lett.* **128**, 213901 (2022).
24. Baudin, K. et al. Observation of light thermalization to negative-temperature Rayleigh-Jeans equilibrium states in multimode optical fibers. *Phys. Rev. Lett.* **130**, 063801 (2023).
25. Ren, H. et al. Nature of optical thermodynamic pressure exerted in highly multimoded nonlinear systems. *Phys. Rev. Lett.* **131**, 193802 (2023).
26. Shi, C., Kottos, T. & Shapiro, B. Controlling optical beam thermalization via band-gap engineering. *Phys. Rev. Res.* **3**, 033219 (2021).
27. Ferraro, M., Mangini, F., Zitelli, M. & Wabnitz, S. On spatial beam self-cleaning from the perspective of optical wave thermalization in multimode graded-index fibers. *Adv. Phys.: X* **8**, 2228018 (2023).
28. Picozzi, A. Towards a nonequilibrium thermodynamic description of incoherent nonlinear optics. *Opt. Express* **15**, 9063–9083 (2007).
29. Kirsch, M. S. et al. Observation of Joule–Thomson photon-gas expansion. *Nat. Phys.* **21**, 214–220 (2025).
30. Podivilov, E. et al. Thermalization of orbital angular momentum beams in multimode optical fibers. *Phys. Rev. Lett.* **128**, 243901 (2022).

31. Ramos, A., Fernández-Alcázar, L., Kottos, T. & Shapiro, B. Optical phase transitions in photonic networks: a spin-system formulation. *Phys. Rev. X* **10**, 031024 (2020).
32. Weidemann, S. et al. Topological funneling of light. *Science* **368**, 311–314 (2020).
33. Haus, H. A. Waves and fields in optoelectronics. *Opt. Acta: Int. J. Opt.* **32**, 748 (1984).
34. Lu, L., Joannopoulos, J. D. & Soljačić, M. Topological photonics. *Nat. Photonics* **8**, 821–829 (2014).
35. Vakil, A. & Engheta, N. Transformation optics using graphene. *Science* **332**, 1291–1294 (2011).
36. Plotnik, Y. et al. Experimental observation of optical bound states in the continuum. *Phys. Rev. Lett.* **107**, 183901 (2011).
37. Kildishev, A. V., Boltasseva, A. & Shalaev, V. M. Planar photonics with metasurfaces. *Science* **339**, 1232009 (2013).
38. Hsu, C. W. et al. Observation of trapped light within the radiation continuum. *Nature* **499**, 188–191 (2013).
39. Yu, Z. & Fan, S. Complete optical isolation created by indirect interband photonic transitions. *Nat. Photonics* **3**, 91–94 (2009).
40. Alù, A. & Engheta, N. Achieving transparency with plasmonic and metamaterial coatings. *Phys. Rev. E* **72**, 016623 (2005).
41. Bar-Hillel, L. et al. Time refraction and time reflection above critical angle for total internal reflection. *Phys. Rev. Lett.* **132**, 263802 (2024).
42. Brongersma, M. L. & Shalaev, V. M. The case for plasmonics. *Science* **328**, 440–441 (2010).
43. Lederer, F. et al. Discrete solitons in optics. *Phys. Rep.* **463**, 1–126 (2008).
44. Kivshar, Y. S. & Campbell, D. K. Peierls–Nabarro potential barrier for highly localized nonlinear modes. *Phys. Rev. E* **48**, 3077 (1993).
45. Stegeman, G. I. & Segev, M. Optical spatial solitons and their interactions: universality and diversity. *Science* **286**, 1518–1523 (1999).
46. Chen, H.-H. & Liu, C.-S. Solitons in nonuniform media. *Phys. Rev. Lett.* **37**, 693 (1976).
47. Peschel, U., Pertsch, T. & Lederer, F. Optical Bloch oscillations in waveguide arrays. *Opt. Lett.* **23**, 1701–1703 (1998).
48. Morandotti, R., Peschel, U., Aitchison, J., Eisenberg, H. & Silberberg, Y. Experimental observation of linear and nonlinear optical Bloch oscillations. *Phys. Rev. Lett.* **83**, 4756 (1999).
49. Agrawal, G. P. in *Nonlinear Science at the Dawn of the 21st Century* (eds Christiansen, P. L. et al.) 195–211 (Springer, 2000).

[1]Ming Hsieh Department of Electrical and Computer Engineering, University of Southern California, Los Angeles, CA, USA. [2]Abbe Center of Photonics, Friedrich Schiller University Jena, Jena, Germany. [3]Department of Physics and Astronomy, University of Southern California, Los Angeles, CA, USA. [4]These authors contributed equally: Hediyeh M. Dinani, Georgios G. Pyrialakos. ✉e-mail: demetri@usc.edu; khajavik@usc.edu

Data availability
Source data are provided with this paper. All other data supporting the plots and findings within this paper are available from the corresponding authors upon request.

Code availability
The numerical codes used in this study (MATLAB) are available upon request from the corresponding authors.

Acknowledgements
This research was partially supported by the US Department of Energy, Office of Basic Energy Sciences, Division of Materials Sciences and Engineering (Award No. DE-SC0025224 for developing the theory and building the experimental set-up to H.M.D., A.M.B.B., M.A.S., H.R., G.G.P., D.N.C. and M.K.), Army Research Office (Grant No. W911NF-23-1-0312 to H.M.D., A.M.B.B., M.A.S., H.R., G.G.P., D.N.C. and M.K.), the Air Force Office of Scientific Research (AFOSR) Multidisciplinary University Research Initiative (MURI) (Award No. FA9550-20-1-0322 for novel light–matter interactions in topologically non-trivial Weyl semimetal structures and systems to H.M.D., A.M.B.B., M.A.S., H.R., G.G.P., D.N.C. and M.K.), ONR MURI (Award No. N00014-20-1-2789 for the classical entanglement of light to H.M.D., A.M.B.B., M.A.S., H.R., G.G.P., D.N.C. and M.K.), AFOSR MURI (Award No. FA9550-21-1-0202 for programmable systems with non-Hermitian quantum dynamics to H.M.D., A.M.B.B., M.A.S., H.R., G.G.P., D.N.C. and M.K.), Department of Energy (Grant No. DESC0022282 to M.A.S., H.R., G.G.P. and D.N.C.), W. M. Keck Foundation (M.A.S., H.R., G.G.P. and D.N.C.), the MPS Simons collaboration (Simons Grant No. 733682 to M.A.S., H.R., G.G.P. and D.N.C.), US Air Force Research Laboratory (Grant No. FA86511820019 to M.A.S., H.R., G.G.P. and D.N.C.), and fellowships from the University of Southern California (H.M.D. and A.M.B.B.).

Author contributions
G.G.P., H.M.D., D.N.C. and M.K. developed the idea. H.M.D. and G.G.P. performed the simulations. H.M.D. and A.M.B.B. built the set-up, and H.M.D. performed the experiments. All authors contributed to the analysis of the results and preparation of the paper.

Competing interests
The authors declare no competing interests.

Additional information
Supplementary information The online version contains supplementary material available at https://doi.org/10.1038/s41566-025-01756-4.

Correspondence and requests for materials should be addressed to Demetrios N. Christodoulides or Mercedeh Khajavikhan.

Peer review information *Nature Photonics* thanks Tsampikos Kottos, Maxim Shcherbakov and the other, anonymous, reviewer(s) for their contribution to the peer review of this work.